Reaction kinetics exploration of a protocellular metabolism

Ditlev Hartmann Bornebusch[1,2*], Hans-Joachim Ziock[3*] and Steen Rasmussen[2,4*]

[1]Sino-Danish Center, University of Chinese Academy of Sciences, Beijing, China; [2]FLinT Center, University of Southern Denmark; [3]Los Alamos, NM 87544, U.S.A.; [4]Santa Fe Institute, New Mexico 87501, U.S.A.
*deltaetabeta@gmail.com &*hziock@outlook.com & *steen@sdu.dk

Introduction

The reaction kinetics of a photochemically driven protocell system, previously implemented in the lab[(1)], is explored in simulation to further investigate the requirements for minimal and possible early life reaction systems[(1)-(6)]. The system studied is based on a process in which a subunit of a potentially self-replicable information module supplies the means of producing additional copies of itself, as well as building blocks of a self-assembling container unit with which it associates. The information unit directly participates in a cyclic metabolism that converts resource molecules into building blocks that self-assemble due to their amphiphilic nature.

The photo-driven metabolic network

The reaction kinetic equations corresponding to Fig 1 are:

$$d[R_1]/dt = -k_{hv}[R_1] + k_f[R_2] + k_{be1}[R_3] + k_{reg}[R_4][SH_2] \quad (1)$$
$$d[R_2]/dt = k_{hv}[R_1] - k_f[R_2] - k_{red}[R_2] \quad (2)$$
$$d[R_3]/dt = k_{red}[R_2] - k_{be1}[R_3] - k_{be2}[R_3][L_P] \quad (3)$$
$$d[R_4]/dt = k_{be2}[R_3][L_P] - k_{reg}[R_4][SH_2] \quad (4)$$
$$d[L_P]/dt = -k_{be2}[R_3][L_P] - k_h[L_P] \quad (5)$$
$$d[L_{ep}]/dt = k_{be2}[R_3][L_P] - k_c[L_{ep}] \quad (6)$$
$$d[p\cdot]/dt = k_c[L_{ep}] - k_l[p\cdot][SH_2] \quad (7)$$
$$d[p_H]/dt = k_l[p\cdot][SH_2] \quad (8)$$
$$d[L_e]/dt = k_c[L_{ep}] - k^+_{leq}[L_e][H_p] + k^-_{leq}[L] \quad (9)$$
$$d[L]/dt = k_h[L_P] + k^+_{leq}[L_e][H_p] - k^-_{leq}[L] \quad (10)$$
$$d[H_p]/dt = k_{be2}[R_3][L_P] - k^+_{leq}[L_e][H_p] + k^-_{leq}[L] \quad (11)$$
$$d[P_{OH}]/dt = k_h[L_P] \quad (12)$$
$$d[SH_2]/dt = -k_{reg}[SH_2][R_4] - k_l[SH_2][p\cdot] + k_{sre}[SH\cdot]^2 \quad (13)$$
$$d[SH\cdot]/dt = k_{reg}[SH_2][R_4] + k_l[SH_2][p\cdot] - 2k_{sre}[SH\cdot]^2 \quad (14)$$
$$d[S]/dt = k_{sre}[SH\cdot]^2. \quad (15)$$

Table 1: Rate constants and their estimated values

Symbol	Name/Role	Nominal value
k_{hv}	photoexcitation (inc. light int. & abs.)	4.800×10^{-1} /s
k_f	fluorescence decay of excited catalyst	6.930×10^{5} /s
k_{red}	reductive quench of excited catalyst	6.930×10^{4} /s
k_{be1}	back electron to give catalyst ground state	1.000×10^{8} /s
k_{be2}	(initial) electron transfer to lipid precursor	2.933×10^{8} /M·s
k_{reg}	regeneration of R_1 from R_4	1.000×10^{6} /M·s
k_l	picolyl waste deradicalization	1.000×10^{6} /M·s
k_c	cleavage of L_P after e^- transfer	1.000×10^{0} /s
k_h	(initial) hydrolysis cleavage of L_P	4.500×10^{-6} /s
k^+_{leq}	reformation of decanoic acid	1.000×10^{8} /M·s
k^-_{leq}	dissociation of decanoic acid	1.000×10^{6} /s
k_{sre}	disproportionation to regenerate SH_2	1.000×10^{6} /M·s

To explore the possibilities and limitations of the involved metabolic network, we analyze the simplest version of the previously implemented metabolic network[(1)].

In the metabolic network (Fig. 1), container building blocks (decanoic acid: L + L_e) are generated from precursor molecules (picolinium esters: L_P) driven by photolysis (light energy) by photosensitizer (ruthenium-tris-bipyridine: $Ru(bpy)_3$). This is covalently bound to a particular nucleobase (8-oxo-

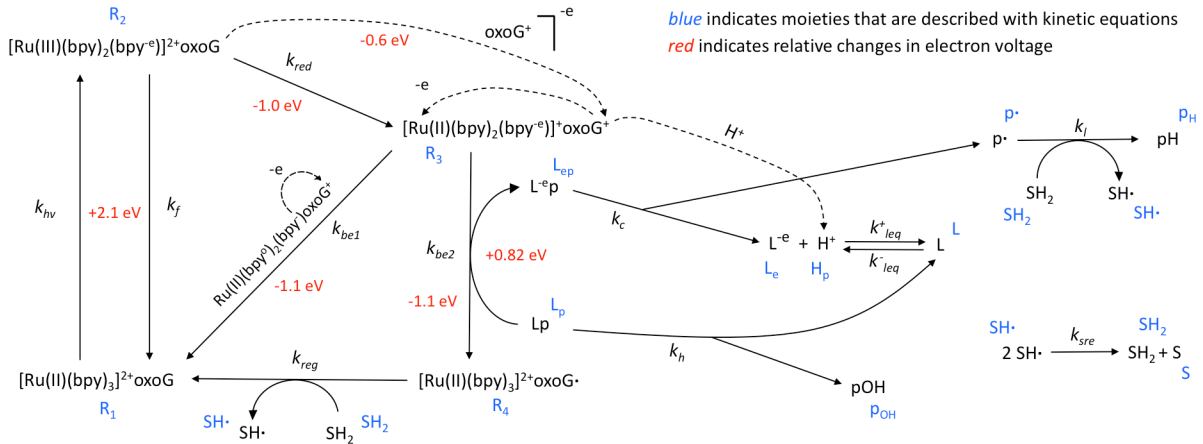

Figure 1: Reaction kinetics scheme. Initial concentrations are: $R_1 = 1\times10^{-3}$ M, $L_P = 15\times10^{-3}$ M; $SH_2 = 15.75\times10^{-3}$ M. The corresponding reaction kinetic equations are given in the text and their rate constants estimates in Table 1. Rate constants estimates are in part based on direct analysis of experimental data and in part on simulations. Note that only oxoG (and not G) has sufficient redox potential to allow the photocatalytic reaction to proceed. The dotted line from oxoG to $oxoG^+$ indicates that an electron is separated from oxoG, while the two dotted lines from $oxoG^+$ respectively indicate where the separated electron and the successive separated proton go. Dotted line at k_{be2} path shows back electron. See text for details.

guanine: oxoG) that acts as an electron donor to the photoexcited $Ru(bpy)_3$, so that photoexcited electrons are available to "digest" (cleave) the precursors L_P that result in the formation of container building blocks ($L + L_e$).

Key reaction parameter estimation

The photoexcitation of the ruthenium complex is the first reaction to estimate in Fig 1. From ref. (1) we get the photoexcitation rate (EX) is calculated as (photons/(s·cm^2)) / (molecules of photocatalyst / cm^2) and is EX = 0.48 (photon/molecule)/s = k_{hv}. The initial overall fatty acid production rate is measured to be 2.1×10^{-6} M/s; therefore from 0.001 M Ru the turnover rate is 2.1×10^{-6} M/s / 0.001 M = 2.1×10^{-3}/s. This gives a photoexcitation rate of 0.48 (photon/molecule)/s of the excited Ru complex yielding 2.1×10^{-3} fatty acid molecules per second. This defines a photoexcitation/quantum yield PY of

$$PY = (2.1\times10^{-3}\, s^{-1}) / (0.48\, s^{-1}) = 0.0044. \quad (16)$$

The photocatalysis route leading to lipid production has a pair of branching points k_{red} vs. k_f (where the k_{red} branch needs to be chosen) followed by k_{be2} vs. k_{be1}, where the k_{be2} pathway must be chosen for lipid production to occur. These two bifurcation pathways for the electron transfer process give relative sizes of k_{red}/k_f and $(k_{be2}\,[L_P(0)])/k_{be1}$, where $[L_P(0)] = 1.5\times10^{-2}$ M is the initial concentration of L_P. This means

$$(k_{red}/k_f) \times (k_{be2}\, 1.5\times10^{-2}\,\mathrm{M})/k_{be1}) = 0.0044. \quad (17)$$

It is further stated that the quenching of the oxo-G is less than or equal to 10%.[1] This implies $k_{red}/k_f \sim 0.1$ and ($k_{be2}\times1.5\times10^{-2}$ M) / $k_{be1} \sim 0.044$) as Eq. (17) needs to be satisfied. From this we can estimate that

$$k_{be2}/k_{be1} = 0.044\ /(1.5\times10^{-2}\mathrm{M}) = 2.933/\mathrm{M}. \quad (18)$$

Ref. (1) SI also has experimental information about the hydrolysis reaction that we can use to approximate k_h. Guanine (G, as opposed to oxoG) does not have a sufficient redox potential to allow the photocatalytic reaction to proceed, leaving only the hydrolysis reaction (the k_h term in Eq. (5)) to produce lipid. Keeping only this term in Eq. (5), the modified equation takes on a form whose solution is a decreasing exponential, $[L_P(t)] = [L_P(0)]\exp(-k_h t)$. From a 1st order Taylor expansion of $\exp(-k_h t)$ and since $[L_P(0)] - [L_P(t)] \approx ([L(t)] + [L_e(t)])$, we get $([L(t)]+[L_e(t)]) / [L_P(0)] \approx k_h\, t$, or an initial linear dependence of fractional lipid production with time. From this and the initial Fig. 2 guanine curve slope, we find $k_h \approx 4.5\times10^{-6}$/s.

Reaction kinetic simulations

MATLAB software was used to numerically solve the coupled set of Eqs. (1-15) with the starting concentrations used in Ref. (1), all while exploring a range of values of the rate constants centered on the nominal values given in Table 1. As noted above, we have good values for k_{hv} and k_h, as well as for the ratios of k_{be2}/k_{be1} and k_{red}/k_f and their product, so these values were kept constant. The values for $([L(t)]+[L_e(t)])$ are compared to the experimental values of Fig. 3 in Ref. (1) SI in order to judge the appropriateness of the values explored.

Fits are typically quite good at early times, but later the experimental data fall well below the simulations, see Fig. 2. We speculate that this is due to the formation of molecular structures that in different ways inhibit the hydrolysis reaction and electron transfer from R_3 to the precursor. We assume a slow

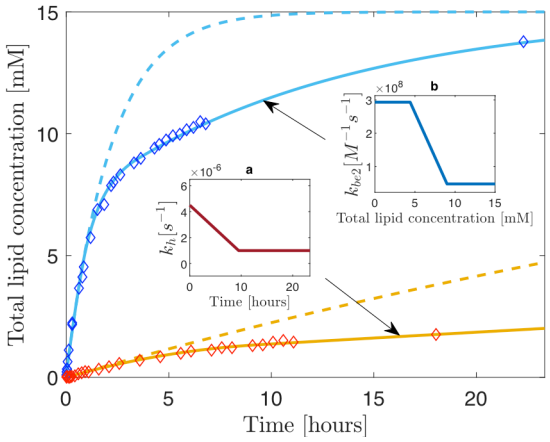

Figure 2: Diamonds are datapoints from experimental data[1]; blue = oxoG and red = G reaction. Solid lines are corresponding simulations. Dotted lines are simulations without rate constant corrections due to structure formation. *Inset* (a): Approximation of precursor availability for hydrolysis due to L_P droplet aggregation that decreases k_h over time. *Inset* (b): Approximation of vesicle and membrane formation that impacts the availability of precursor L_P for photofragmentation. Fatty acid structure formation starts above 4 mM that coats the precursor L_P. This process insulates the precursor from the Ru complex and photocatalysis, which decreases k_{be2} depending on lipid concentration level.

droplet formation dominates in the G experiment that decreases droplet surface and hydrolysis, implying a slow decrease of k_h until a stable lower hydrolysis level is eventually reached, see Fig. 2 (a). For the oxoG experiment, we assume rapid fatty acid structure formation above the CVC (>4 mM) causes a membrane coating of the available L_P. This insulates the photocatalyst from the precursor and thereby lowers the photocatalysis rate k_{be2} until a lower catalysis level is reached at a high lipid concentration. For simplicity, in the oxoG simulation, we use a constant average $k_h = 2.5\times10^{-6}$/s. The function insets (a) and (b) in Fig. 2 are the simplest we could identify that enables the simulations to match the experimental data.

Discussion and Outlook

A simple reaction kinetic analysis provided us with valuable information about how the metabolic network operates. Notably, the values of most of the rate constants can be changed by several orders of magnitude provided ratios k_{red}/k_f and $(k_{be2}\,[L_P(0)])/k_{be1}$, as well as the k_{hv} and k_h values are maintained. Part of this insensitivity is explained by the small value of k_{hv}, which means that smaller or larger values of many of the rate constants make no difference. In any event, added experiments are needed to identify the actual values. Rate constant estimates based on current knowledge are given in Table 1. Clearly, the emergence of aggregates slows down the fatty acid production, while these lower rate constants seem to be steady (and lower) once the aggregates have fully formed.

Our metabolic network also functions for DNA oligomers ligation as demonstrated in Ref. (3). Further, the metabolic network functions when the oxoG is separated from the Ru complex as demonstrated in Ref. (2). This is critical for a future incorporation of the oxoG into a self-replicating information system, which is outlined in Ref (4). How to circumvent product inhibition in the ligation based self-replication process is discussed in Refs. (5) and (6).

References

1) DeClue, M.S., Monnard, P.-A., Bailey, J., Maurer, S.E., Collins, G.E., Ziock, H.J., & Rasmussen, S. (2009). Nucleobase Mediated, Photocatalytic Vesicle Formation from Ester Precursor Molecules. *JACS*, 131, 3, 931–933.

2) Maurer, S.E., DeClue, M.S., Albertsen, A.N., Dçrr, M., Kuiper, D.S., Ziock, H., S., Boncella, J.M., Monnard, P.-A. (2011). Interactions between Catalysts and Amphiphilic Structures and their Implications for a Protocell Model. *ChemPhysChem,* 12, 828–835.

3) Cape, J.L., Edson, J.B., Spencer, L.P., DeClue, M.S., Ziock, H.-J., Maurer, S., Rasmussen, S., Monnard, P.-A., & Boncella, J.M. (2012). Phototriggered DNA Phosphoramidate Ligation in a Tandem 5′-Amine Deprotection/3′-Imidazole Activated Phosphate Coupling Reaction. *Bioconjug. Chem.* 23, 2014–2019.

4) Rasmussen, S., Constantinescu, A., and Svaneborg, C. (2016). Generating minimal living systems from nonliving materials and increasing their evolutionary abilities. *Phil. Trans. Royal Soc. B.* 1701:371.

5) Engelhardt J., Andersen B., and Rasmussen, S. (2020). Thermodynamics and kinetics of Lesion Induced DNA Amplification (LIDA). In Bongard, J., Lovato, J., Hebert-Dufrésne, L., Dasari, R., and Soros, L., editors, *Artificial Life 2020*, pages 269–272. MIT Press, Cambridge, MA.

6) Bornebusch, D.H., Sørensen C.C., Zingg P., Gazzola G., Packard N., and Rasmussen S. (2020). Automated replication optimization for protocellular information system. In Bongard, J., Lovato, J., Hebert-Dufrésne, L., Dasari, R., and Soros, L., editors, *Artificial Life 2020*, pages 219–220. MIT Press, Cambridge, MA.